

One-step synthesis of colloidal $\text{CH}_3\text{NH}_3\text{PbBr}_3$ nanoplatelets via chlorobenzene to realize nonsolvent crystallization

Hao Zheng^{1,2} , Wei Pan^{1,2,3}  and Wenzhong Shen^{1,2,3}

¹Laboratory of Condensed Matter Spectroscopy and Opto-Electronic Physics, Shanghai Jiao Tong University, Shanghai 200240, People's Republic of China

²Key Laboratory of Artificial Structures and Quantum Control (Ministry of Education), School of Physics and Astronomy, Shanghai Jiao Tong University, Shanghai 200240, People's Republic of China

E-mail: sjtushelwill@sjtu.edu.cn and wzshen@sjtu.edu.cn

Received 4 May 2018, revised 10 August 2018

Accepted for publication 23 August 2018

Published 7 September 2018



CrossMark

Abstract

Ligand-assisted reprecipitation (LARP) is a convenient and low-cost method to synthesize perovskite nanoplatelets (NPLs) with great optoelectronic properties. However, it still suffers from delicate purification and passivation. Here, we report the synthesis of perovskite NPLs via a simple one-step method through using chlorobenzene as poor solvent. These as-prepared NPLs exhibit good lateral-size homogeneity and emission wavelength tunability. Controlled experiment indicates that compared to the commonly used toluene, chlorobenzene is advantaged to enhance photoluminescence quantum yield (PLQY) and decay time of the perovskite NPLs. Raman spectra, x-ray photoelectron spectroscopy and energy dispersive spectra have shown that it is the passivation of chlorine atoms which suppresses nonradiative recombination and enhances PLQY. These results demonstrate that chlorobenzene is an alternative poor solvent to realize both the simplification of the LARP technique and the passivation of perovskite NPLs.

Supplementary material for this article is available [online](#)

Keywords: LARP, perovskites, chlorobenzene, passivation, NPLs

(Some figures may appear in colour only in the online journal)

1. Introduction

Perovskite nanocrystals (NCs) have emerged as promising materials in light-emitting devices (LED) due to their excellent optoelectronic properties, easy to solution process, and broad wavelength tunability [1–4]. Compared to cubic NCs, perovskite nanoplatelets (NPLs) show stronger quantum confinement and anisotropic emission, which is beneficial to controlling emission homogeneity and increasing the light outcoupling efficiency and LED efficiency [5]. Several synthetic approaches have been applied to prepare perovskite

NPLs, such as hot injection, ligand-assisted reprecipitation (LARP), and exfoliation method [6–11]. Among them, LARP has attracted public attention for its convenience and low-cost.

In LARP method, the perovskite colloidal NPLs were crystallized at room temperature through solubility change of precursors by mixing a pair of good and poor solvents. However, LARP method still has some problems. As-prepared products generally contain not only broadly size-distributed nanoparticles, but some bulk-like materials [5, 12]. As a result, a further purification step is necessary to separate the homogeneous NPLs. Compared to classical NPLs, perovskites are more ionic in nature, so that polar solvent usually

³ Authors to whom any correspondence should be addressed.

Table 1. Details of the synthesis, PL peaks, $\tau_{1/e}$, and PLQY of as-synthesis PhCl and purified toluene samples.

Sample name	PhCl samples				Toluene samples			
	PLQY %	$\tau_{1/e}$ ns	PL peaks nm	OAm μ l	PL peaks nm	$\tau_{1/e}$ ns	PLQY %	Sample name
PhCl-452	28	12.3	452	16	452	5.8	19	Tol-452
PhCl-470	33	14.6	470	18.5	468	10.3	26	Tol-468
PhCl-482	39	19.2	482	21	487	13.9	31	Tol-487
PhCl-501	47	24.1	501	24	496	15.9	33	Tol-496
PhCl-526	62	40.0	526	30	535	23.4	45	Tol-535

induces photoluminescence (PL) quenching or even destroys the perovskite NPLs [13, 14]. Common purification techniques are failed to purify perovskite NPLs, and the special purification is very delicate and challenging [7, 12]. For example, a mixture solution with certain ratio of acetonitrile/toluene has been used as washing solvents to avoid decomposition of NPLs [7]. Several cycles of washing treatment with hexane/ethyl acetate mixed solvent were also proposed to maintain sufficient surface ligand density and stabilize the NPLs in solution [14]. Therefore, a simple purification process, and even an optimized reprecipitation technique is needed to be explored.

On the other hand, low synthetic temperature, as well as the high surface-volume ratio of NPLs, easily leads to the existence of high-density structure defects and trap states. Therefore, the passivation engineering is also a key issue, which has been studied by previous work [15–17]. For example, peptides with amino and carboxylic functional groups dissolved in precursor solution were used as passivating ligands to produce well-passivated perovskite NCs [15]. The replacement of coordinated N,N-Dimethylformamide (DMF) with noncoordinated acetonitrile as a good solvent could also avoid the formation of solvent intermediates and intrinsic halide vacancies, and finally realize a stronger emission and stable $\text{CH}_3\text{NH}_3\text{PbI}_3$ quantum dots [16].

To the best of our knowledge, it is still difficult to realize both the direct optimization and passivation by poor solvent in LARP. Here, we report a one-step synthesis of perovskite NPLs by using chlorobenzene (PhCl) as poor solvent, which is a commonly used antisolvent in perovskite film fabrication to enhance film quality [18–20]. Controlled experiments demonstrate that compared to those made by toluene, the samples synthesized from PhCl exhibit better dispersity, more uniform lateral size distribution, and higher photoluminescence quantum yield (PLQY). Furthermore, within whole emission tunable range (452–526 nm), the products exhibit higher PLQY and longer decay time. Further studies have indicated that the improvement of PLQY comes from the suppression of the defect-related nonradiative recombination. Raman spectra, x-ray photoelectron spectroscopy (XPS), and energy dispersive spectra (EDS) suggest the existence of defect passivation by Cl atom. Obviously, using PhCl as poor solvent not only simplifies the synthesis to one-step, but directly passivates the defects of as-synthesized NPLs.

2. Experimental section

2.1. Chemicals

Lead bromide (PbBr_2 , 99.99%) and methylammonium bromide ($\text{CH}_3\text{NH}_3\text{Br}$, 99.5%) were purchased from Xi'an Polymer Light Technology Corp. Oleic acid (OAc, 99%), oleylamine (OAm, 80%–90%) and chlorobenzene (PhCl, anhydrous, 99.5%) were purchased from Aladdin. Toluene (anhydrous, 99.8%) and DMF (anhydrous, 99.8%) were purchased from Sigma-Aldrich.

2.2. Synthesis of $\text{CH}_3\text{NH}_3\text{PbBr}_3$ perovskite colloidal NPLs

Colloidal perovskite NPLs were prepared via the LARP method proposed by Levchuk *et al* with a little modification [7]. All the synthetic procedures were performed at room temperature in the glovebox under nitrogen atmosphere.

In a typical synthesis, 0.1 mmol of $\text{CH}_3\text{NH}_3\text{Br}$, 0.1 mmol of PbBr_2 , 0.2 ml of OAc, and 16 μ l of OAm were added into a 1 ml of DMF (good solvent) to form the precursor solution. The precursor solution was sonicated for 15 min. Then, 100 μ l of the precursor solution was added dropwisely to 3 ml of vigorously stirred PhCl (poor solvent) and maintained for 5 min to precipitate $\text{CH}_3\text{NH}_3\text{PbBr}_3$ NPLs. The as-prepared $\text{CH}_3\text{NH}_3\text{PbBr}_3$ NPLs emitted bright green light.

To realize the different emission wavelength by controlling the size of NCs, the volume of OAm in the precursors was controlled from 16 to 30 μ l. The same precursor was also dispersed dropwisely to 3 ml of toluene (poor solvent) to make a control experiment. Details about the synthesis were listed in table 1.

2.3. Characterization

The transmission electron microscopy (TEM) images were obtained by a JEOL (Japan) JEM-2100 TEM. The high resolution (HR) TEM image was obtained by a Titan (USA) 80-300 TEM. TEM-EDS spectra was acquired by FEI (USA) Talos F200X. Ultraviolet-visible (UV-vis) absorption spectra were measured by Thermo Electron (USA) EV300. PL spectra and the absolute PLQY were obtained from a fluorescence Spectro fluorometer equipped with an integrating sphere accessory (Horiba Jobin Yvon, FL, Japan). PL decay curves were collected by exciting the perovskite colloidal dispersions with a pulse laser at 375 nm (Horiba Jobin Yvon,

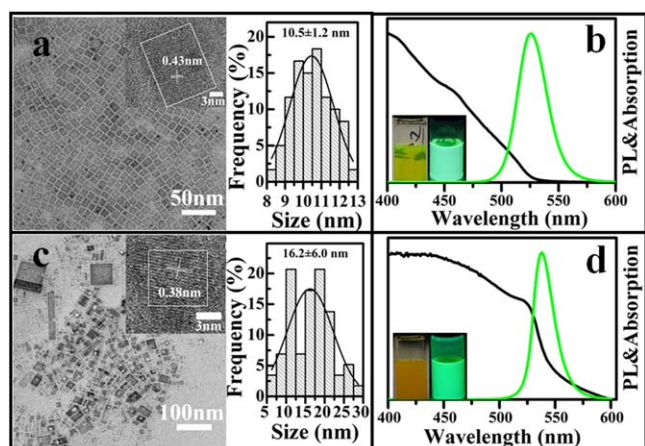


Figure 1. (a), (c) Typical TEM and size distribution, (b), (d) PL and UV-vis absorption spectra of as-prepared $\text{CH}_3\text{NH}_3\text{PbBr}_3$ NPLs synthesized with $16 \mu\text{l}$ of OAm. The top figures are PhCl sample while the bottom figures correspond to toluene sample. The inset of (a) and (c) are the HRTEM images. The inset of (b) and (d) are corresponding photographs under the illumination of daylight and UV (365 nm) light.

FL, Japan). The photographs were taken by a Nikon D5300 camera under the illumination of room light and UV light (365 nm). For XPS and Raman spectra measurements, the samples were added with 1.5 ml of acetonitrile and centrifuged at 10 000 rpm for 3 min. The precipitates were transferred onto the silicon substrate and dried in vacuum for 12 h. XPS spectra were recorded by AXIS Ultra DLD (Japan) XPS. Raman spectra were performed by dispersive Raman microscope (Senterra R200-L, German) with 633 nm laser light.

3. Results and discussion

The synthesis of $\text{CH}_3\text{NH}_3\text{PbBr}_3$ NPLs were realized by the crystallization of precursors in the poor solvent. Previous work commonly selected toluene as poor solvent, accompanied by further centrifugation and washing process to obtain bright and uniform-size NCs [7, 16, 21]. Here, we choose PhCl as poor solvent to realize one-step synthesis which omits the further cleaning procedure. To make a control experiment, toluene is also selected as poor solvent to prepare $\text{CH}_3\text{NH}_3\text{PbBr}_3$ NPLs. For both two solvents, the crystallization occurred immediately and the solutions exhibited green fluorescence.

Figures 1(a) and (c) show TEM images of perovskite NPLs precipitated in PhCl and toluene, respectively. Both NPLs of PhCl and toluene samples are sheet-shaped crystals, with a lattice spacing of 0.43 and 0.38 nm respectively, as observed from HRTEM images in the inset of figures 1(a) and (c). These images also clearly demonstrate that PhCl samples have good size homogeneity, but toluene samples have a larger size distribution from small to giant NPLs. Statistical analysis of TEM images gives a Gaussian lateral size distribution of 10.5 ± 1.2 nm for PhCl samples, much narrower than that (16.2 ± 6.0 nm) of toluene samples. Figures 1(b)

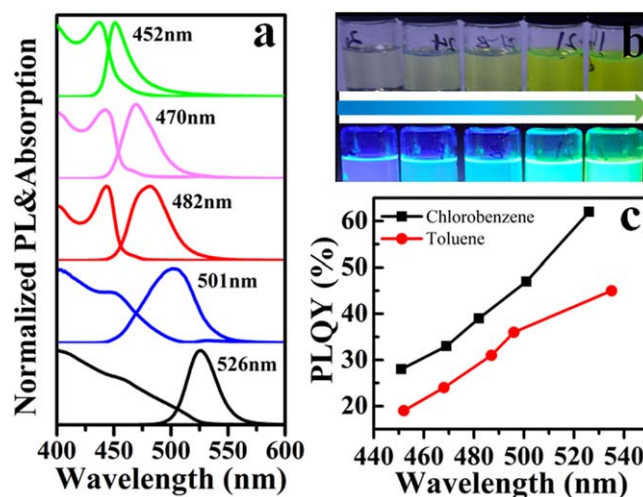


Figure 2. (a) Normalized PL and absorption spectra, (b) photographs under daylight (top) and UV light (bottom) of perovskite colloidal nanocrystal in PhCl synthesized with $16\text{--}30 \mu\text{l}$ of OAm. (c) Absolute PLQY of as-synthesized PhCl samples and purified toluene samples.

and (d) display UV-vis absorption and PL spectra of NPLs dispersed in PhCl and toluene, respectively. Their absorption spectra do not demonstrate an obvious excitonic peak, which may indicate a mixture of NPLs with different perovskite layers [22], in accordance to TEM images with diverse contrast. Under the illumination of 365 nm UV light, the clear PhCl solution emitted bright green light (inset of figure 1(b)), whose PL peak located at 526 nm, with a full-width at half-maxima (FWHM) of 29 nm and a PLQY of 62%. In contrast, the toluene solution was turbid with a lower PLQY of 26%, although it also emitted green light centered at 535 nm with a slightly narrower FWHM of 21 nm. Obviously, the replacement of toluene with PhCl is helpful to synthesize the NPLs with better lateral size homogeneity and higher PLQY.

One possible reason for low PLQY of toluene samples is the aggregation of larger NPLs in solution (see inset of figure 1(d)) since the as-synthesized toluene samples is turbid. The aggregation is disadvantaged to the PLQY which increases the nonradiative recombination and depresses the radiative recombination of photo-excited electron-hole pairs in NPLs. To exclude the influence of aggregation in solution, an additional centrifugation-step (4000 rpm, 2 min) was used to discard larger NPLs in toluene samples. As shown in figure S1, available online at stacks.iop.org/NANO/29/455601/mmedia, clear toluene samples were obtained after large visible agglomerates were removed. This purification step improved the PLQY of toluene sample from 26% to 45%. However, this value was still lower than that (62%) of as-prepared PhCl sample. The use of PhCl as poor solvent not only simplifies the synthesis to one-step method, but also improves the PLQY.

To further explore versatility of PhCl as poor solvent, we varied the amounts of ligand (OAm), and obtained $\text{CH}_3\text{NH}_3\text{PbBr}_3$ NCs with different band gaps and emission wavelengths. As shown in figure 2(a), with the increasing OAm from 16 to $30 \mu\text{l}$, the absorption spectra have changed

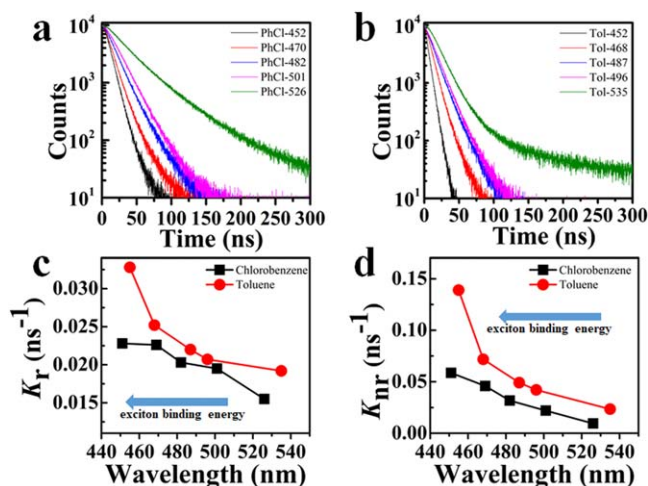


Figure 3. PL decay curves detected at emission maxima for (a) PhCl, and (b) toluene samples with different emissions. (c) Radiative decay rates (K_r), and (d) nonradiative decay rates (K_{nr}) of PhCl samples and toluene samples as a function of emission wavelength.

from a broad absorption behavior to a strong excitonic absorption feature. Correspondingly, PL peak show a gradual blueshift from 526 to 452 nm, which is possibly induced by the stronger quantum confinement effect [3, 23]. The photographs of PhCl samples in figure 2(b) also demonstrate the continuous variation of emission from blue to green. Apparently, besides the widely reported toluene, PhCl acting as poor solvent, is also valid for the synthesis of $\text{CH}_3\text{NH}_3\text{PbBr}_3$ NCs with tunable emission wavelength (452–526 nm). Moreover, the tunable range of PhCl is comparable to those (452–535 nm) of toluene, although the PhCl samples possess a slightly wider PL profile (figures 2(a) and S2).

The PL broadening related thickness uniformity [23], as well as the above-mentioned lateral size homogeneity, mainly originates from the difference of nucleation and growth kinetics induced by dielectric constants of solvent [7]. Compared to toluene ($\epsilon = 2.4$), PhCl possesses larger dielectric constants ($\epsilon = 5.6$), so that it blends faster and better with DMF ($\epsilon = 37.8$). Faster nucleation means that more and smaller crystal seeds are produced at the beginning of solvents-mixing which retard the following growth. According to statistical law, they will induce worse monochromaticity control but is beneficial to lateral size homogeneity.

In figure 2(b), we notice that green samples are brighter than blue samples under UV light, so we performed absolute PLQY measurements for as-synthesized PhCl and purified toluene samples (figure 2(c)). Clearly, for the two series of samples, their PLQY decreases with the blueshift of PL peaks. In details, the PLQY amounts to 62% and 45% for the PhCl-526 and Tol-535, respectively, then it gradually drops to 28% and 19% with the blueshift of PL peaks. This phenomenon is probably from the increase of surface-volume ratio with the decreasing thickness of $\text{CH}_3\text{NH}_3\text{PbBr}_3$. Larger surface-volume ratio means more defects, faster nonradiative decay rate, and thus lower PLQY [7].

Another obvious feature in figure 2(c) is that PhCl samples always show higher PLQYs than toluene samples

within entire color tunable ranges. To gain more insight into it, we acquired their PL decay curves. As shown in figures 3(a) and (b), toluene samples exhibit faster decay than PhCl samples. To compare these decay curves, we define a decay time parameter ($\tau_{1/e}$) as time span dropped to 1/e of the original intensity, as listed in table 1. The decay time of PhCl samples is longer than that of toluene samples synthesized from the same precursor. PL decay is determined by radiative and nonradiative channels with their respective decay time τ_r and τ_{nr} , so that $\frac{1}{\tau_{1/e}} = \frac{1}{\tau_r} + \frac{1}{\tau_{nr}}$. The PLQY also depends on the two channels, as $\text{PLQY} = \frac{\tau_{nr}}{\tau_r + \tau_{nr}}$. Combining two formulas with measured values of $\tau_{1/e}$ and PLQY, we obtain the corresponding radiative ($K_r = 1/\tau_r$) and non-radiative decay rates ($K_{nr} = 1/\tau_{nr}$) of both samples (figures 3(c) and (d)).

These curves exhibit two obvious trends. Firstly, for both PhCl and toluene samples, K_{nr} and K_r increase with the decreasing thickness and the parallel blueshift trend of PL emission. The increasing K_r with decreasing PL emission peaks could be explained by the increasing exciton binding energy induced by the decreasing size of confined dimension and the weakening of screening effect of the Coulomb interaction between electron and holes [3, 23]. The increasing K_{nr} are due to higher concentration of surface traps of thinner NC, which has a bigger surface-volume ratio.

Secondly, for the two series of samples obtained from the same precursor, PhCl samples always show a slightly lower K_r at a magnitude order of 10^{-3} ns^{-1} and a greatly lower K_{nr} at a magnitude order of 10^{-2} ns^{-1} than toluene samples. The lower K_r in PhCl samples is probably caused by the relatively larger dielectric constant of solvent PhCl. Strong polarity of solvents makes quantum dots interact themselves well and in turn leads to a lower PLQY, as widely reported in CdSe quantum dots [24]. The suppression of nonradiative recombination (lower K_{nr}) is possibly related to the decreasing defect states [21], but the detailed mechanism is still unknown.

To investigate the origin of low defect density of PhCl samples, Raman spectra (figure 4(a)) were conducted firstly in low-frequency range, which show the vibrational modes of PbX_6 octahedra. By Gaussian curves fitting, the broad multi-band structures have been decomposed into three most energetic phonon bands, the asymmetric stretching mode of X-Pb-X ($\delta_{as(X-Pb-X)}$), symmetric stretching mode of X-Pb-X ($\nu_{s(X-Pb-X)}$), and symmetric stretching mode of Pb-X ($\nu_{s(Pb-X)}$), respectively [25]. The cumulative fit curves are nicely consistent with experimental results. The fitted Raman peaks of PhCl samples locate at 76, 108, and 138 cm^{-1} , higher than those (74, 102, and 130 cm^{-1}) of toluene samples, as shown in figure 4(b). It indicates that $\text{CH}_3\text{NH}_3\text{PbBr}_3$ crystallized in PhCl shows a blueshift for each distinguished vibration between lead and halogen atom.

According to the harmonic oscillator model, higher vibrating frequency means smaller reduced mass of vibrating atoms. Therefore, the reduced mass of vibrating atoms in PhCl samples is smaller than that in toluene samples, when assuming same bond strength for all halides [25, 26].

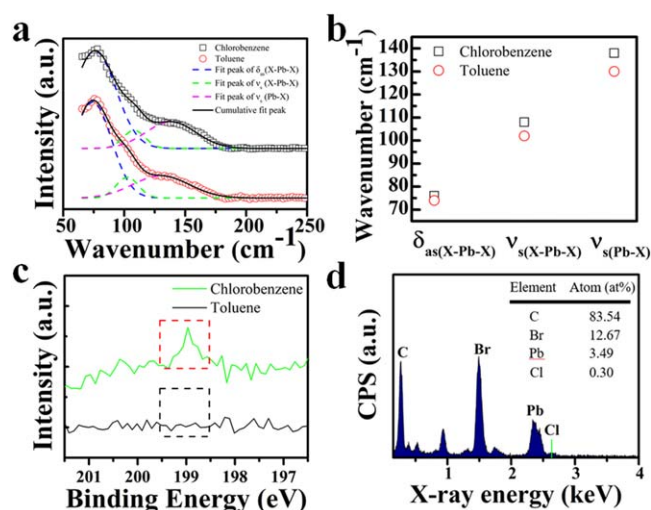


Figure 4. (a) Raman spectra, (b) Raman vibration mode position, and (c) narrow scan XPS spectra of Cl2p core level for PhCl and toluene samples. (d) TEM-EDS spectra and relative atom concentration of C, Br, Pb and Cl for the PhCl samples.

Considering the relationship of $\frac{1}{\mu} = \frac{1}{m_{\text{Pb}}} + \frac{1}{m_{\text{X}}}$ among reduced mass, the mass of vibrating lead and halide atom, the atoms participating into the vibration in PhCl samples have a lighter average mass when compared to toluene samples. It suggests the formation of Pb–Cl bonds in PhCl samples through the Cl passivation of halide vacancies, since previous report has pointed out that DMF as the coordinated solvent is easy to form a defective crystal with residual solvents on the surface and intrinsic halide vacancies [16].

To further confirm the presence of Cl in PhCl samples, we conduct the EDS and XPS measurements for both two samples. As shown in respective full-scan spectra (figure S3), both samples exhibit the obvious peaks of N1s, C1s, Pb4f and Br3d in the perovskite NCs. Further narrow scan spectra of Cl2p core level in figure 4(c) demonstrate a small but recognizable peak at 198.9 eV in PhCl samples, which corresponds to the binding energy position of Cl2p_{3/2} core level [27], suggesting the existence of Pb–Cl bond. The accompanied peak of Cl2p_{1/2} at 200.5 eV is weaker than Cl2p_{3/2}, thus difficult to be directly detected. In addition, EDS analysis in figure 4(d) also proves the existence of chlorine with an atom content of 0.30%, much less than Br atom content of 12.67%. Based on above Raman, XPS and EDS results, we sufficiently verify that Cl is doped in PhCl samples with a relatively low level. These Cl atoms just passivate the halide vacancies rather than influence original crystal structure. The passivation suppresses the nonradiative recombination and prolong the recombination lifetime, resulting in a better PLQY of PhCl samples made by one-step method.

4. Conclusions

In summary, we realize a one-step LARP method for CH₃NH₃PbBr₃ NPLs by selecting PhCl as poor solvent. The replacement of toluene with PhCl promotes the as-synthesized

NPLs with better dispersity, more uniform lateral size and higher PLQY. Even compared to the aggregation-removed toluene samples, PhCl samples still exhibit higher PLQY and longer decay time. The improvement is attributed to suppression of nonradiative recombination by passivation of Cl, as confirmed by Raman spectra, XPS and EDS. This work opens an avenue for solvent selection in LARP to realize a simple, versatile and effective synthesis of perovskite NPLs.

Acknowledgments

This work was supported by the National Natural Science Foundation of China (Grant Nos. 11834011, 11674225 and 11474201).

ORCID iDs

Hao Zheng <https://orcid.org/0000-0003-3034-2397>

Wei Pan <https://orcid.org/0000-0001-7686-6079>

References

- [1] Huang H, Zhao F, Liu L, Zhang F, Wu X-G, Shi L, Zou B, Pei Q and Zhong H 2015 *ACS Appl. Mater. Interfaces* **7** 28128–33
- [2] Protesescu L, Yakunin S, Bodnarchuk M I, Bertolotti F, Masciocchi N, Guagliardi A and Kovalenko M V 2016 *J. Am. Chem. Soc.* **138** 14202–5
- [3] Hintermayr V A, Richter A F, Ehrhart F, Döblinger M, Vanderlinden W, Sichert J A, Tong Y, Polavarapu L, Feldmann J and Urban A S 2016 *Adv. Mater.* **28** 9478–85
- [4] Weidman M C, Seitz M, Stranks S D and Tisdale W A 2016 *ACS Nano* **10** 7830–9
- [5] Weidman M C, Goodman A J and Tisdale W A 2017 *Chem. Mater.* **29** 5019–30
- [6] Bekenstein Y, Koscher B A, Eaton S W, Yang P and Alivisatos A P 2015 *J. Am. Chem. Soc.* **137** 16008–11
- [7] Levchuk I, Herre P, Brandl M, Osvet A, Peukert R H W, Schweizer P, Spiecker E, Batentschuk M and Brabec C J 2016 *Chem. Commun.* **53** 244–7
- [8] Yang S, Niu W, Wang A-L, Fan Z, Chen B, Tan C, Lu Q and Zhang H 2017 *Angew. Chem., Int. Ed. Engl.* **56** 4252–5
- [9] Kirakosyan A, Kim J, Lee S W, Swathi I, Yoon S-G and Choi J 2017 *Cryst. Growth Des.* **17** 794–9
- [10] Shamsi J, Dang Z, Bianchini P, Canale C, Stasio F D, Brescia R, Prato M and Manna L 2016 *J. Am. Chem. Soc.* **138** 7240–3
- [11] Niu W, Eiden A, Prakash V and Baumberg J J 2014 *Appl. Phys. Lett.* **104** 171111
- [12] Shan Q, Song J, Zou Y, Li J, Xu L, Xue J, Dong Y, Han B, Chen J and Zeng H 2017 *Small* **13** 1701770
- [13] Yang G-L and Zhong H-Z 2016 *Chin. Chem. Lett.* **27** 1124–30
- [14] Li J *et al* 2017 *Adv. Mater.* **29** 1603885
- [15] Luo B, Naghadeh S B, Allen A L, Li X and Zhang J Z 2017 *Adv. Funct. Mater.* **27** 1604018
- [16] Zhang F, Huang S, Wang P, Chen X, Zhao S, Dong Y and Zhong H 2017 *Chem. Mater.* **29** 3793–9
- [17] Quan L N, Quintero-Bermudez R, Voznyy O, Walters G, Jain A, Fan J Z, Zheng X, Yang Z and Sargent E H 2017 *Adv. Mater.* **29** 1605945

- [18] Paek S, Schouwink P, Nefeli Athanasopoulou E, Cho K T, Grancini G, Lee Y, Zhang Y, Stellacci F, Nazeeruddin M K and Gao P 2017 *Chem. Mater.* **29** 3490–8
- [19] Zhang X, Wang W, Xu B, Liu S, Dai H, Bian D, Chen S, Wang K and Sun X W 2017 *Nano Energy* **37** 40–5
- [20] Yu J C, Kim D W, Kim D B, Jung E D, Lee K-S, Lee S, Nuzzo D D, Kim J-S and Song M H 2017 *Nanoscale* **9** 2088–94
- [21] Zhang F, Zhong H, Chen C, Wu X-gang, Hu X, Huang H, Han J, Zou B and Dong Y 2015 *ACS Nano* **9** 4533–42
- [22] Yuan Z, Shu Y, Xin Y and Ma B 2016 *Chem. Commun.* **52** 3887–90
- [23] Tong Y, Ehrat F, Vanderlinden W, Cardenas-Daw C, Stolarczyk J K, Polavarapu L and Urban A S 2016 *ACS Nano* **10** 10936–44
- [24] Jose R, Ishikawa M, Thavasi V, Baba Y and Ramakrishna S 2008 *J. Nanosci. Nanotechnol* **8** 5615–23
- [25] Niemann R G, Kontos A G, Palles D, Kamitsos E I, Kaltzoglou A, Brivio F, Falaras P and Cameron P J 2016 *J. Phys. Chem. C* **120** 2509–19
- [26] Ledinský M, Löper P, Niesen B, Holovský J, Moon S-J, Yum J-H, De Wolf S, Fejfar A and Ballif C 2015 *J. Phys. Chem. Lett.* **6** 401–6
- [27] Chen Q *et al* 2015 *Nat. Commun.* **6** 7269